ELECTRON TEMPERATURE VERSUS LASER INTENSITY TIMES WAVELENGTH SQUARED: A COMPARISON OF THEORY AND EXPERIMENTS

R. RAMIS, J.R. SANMARTÍN
E.T.S. Ingenieros Aeronáuticos,
Universidad Politécnica de Madrid,
Madrid,
Spain

ABSTRACT. The peak temperature in the corona of plasma ejected by a laser-irradiated slab is discussed in terms of a one-electron-temperature model. Both heat-flux saturation and pulse rise-time effects are considered; the intensity in the rising half of the pulse is approximated by a linear function of time, $I(t) \equiv I_0 t/\tau$. The temperature is found to be proportional to $(I_0 \lambda^2)^{2/3}$ and a function of $I_0 \lambda^4/\tau$. Above a certain value of $I_0 \lambda^4/\tau$, the plasma presents two characteristic temperatures (at saturation and at the critical surface) which can be identified with experimentally observed cold- and hot-electron temperatures. The results are compared with extensive experimental data available for both Nd and CO_2 lasers, $I_0(W \cdot cm^{-2}) \lambda^2$ (μm) starting around 10^{12}. The agreement is good if substantial flux inhibition is assumed (flux-limit factor $f \cong 0.03$), and fails for $I_0 \lambda^2$ above 10^{15}. Results for both ablation pressure and mass ablation rate are also given.

1. INTRODUCTION

Experiments on the interaction of intense, short laser pulses with solid slabs were performed in many laboratories in the last ten years, as a step preceding the study of spherical-target irradiation for laser fusion. It has been claimed [1, 2] that the available data fall into a universal curve, relating the maximum electron temperature (T_M) during the pulse to the peak light intensity (I_0) times its squared wavelength (λ^2). In a log T_M – log $(I_0 \lambda^2)$ plot, the curve appears to consist of straight segments, with sharp breaks in the slope; above some value of $I_0 \lambda^2$, T_M branches off into 'cold', T_C, and 'hot', T_H, temperatures [3].

The present work is an attempt to reproduce theoretically the changes in the $T_M(I_0 \lambda^2)$ curve. Actually, the analysis should further explain why the correlation of the data is not quite complete, a fact, which, as we claim, is apparent from the compilation of Ref.[3]. The analysis should also explain why the observations are independent of the target properties, which may differ widely among the experiments. A final point of particular interest is the quantitative understanding of temperature branching.

The central idea of the paper is that time-dependent effects are crucial to the problem, and, therefore, the duration or, better, the rise-time τ of the pulse should enter the discussion from the beginning. A relation such as $T_M(I_0 \lambda^2)$ is basically a quasi-steady one, implying that T_M is independent of the pulse history (i.e. basically independent of the time taken by the light intensity to reach its peak). To discuss unsteady effects in the simplest manner, we consider a linear pulse, $I(t) \equiv I_0 t/\tau$, which could reasonably represent the rising half of a Gaussian pulse. Most experiments have been performed with either Nd ($\lambda \cong 1.06$ μm) or $CO_2 (\lambda \cong 10.6$ μm) lasers, τ ranging typically from 0.1 to 1 ns, and from 1 to 10 ns, respectively; I_0, on the other hand, may vary substantially among the laser facilities. If we consider increasing values of I_0, with λ and τ fixed, the pulse steepens, and, at some point, the region between the ablation surface and the surface where the electron density takes its critical value, n_{cr}, is unable to adjust to the rising light intensity in a quasi-steady manner. Our analysis yields a relation $T_M(I_0 \lambda^2, I_0 \lambda^2 \times \lambda^2/\tau)$, weakly dependent on its second argument; the limit $T_M(I_0 \lambda^2, 0)$ would be the quasi-steady regime. For any non-zero λ^2/τ, a weak dependence on λ^2/τ will appear for $I_0 \lambda^2$ large enough.

It appears that target properties do not affect T_M, because of the well defined ablation surface, where the pressure peaks and the density (temperature) is very high (low), compared to the characteristic values in the plasma that expands outside, a fact recently made use of to analyse this region (the corona) in a systematic manner [4—6]. By formally making the ablation

temperature vanish, the corona is decoupled from the part of the target remaining inside the ablation surface. The only material properties entering the description of the coronal plasma are the ion charge number, Z_i, and the mass-to-charge-number ratio, m_i/Z_i.

In Refs [4–6], Spitzer's heat flux was used, on the assumption that the plasma was collision-dominated. Though collisions are frequent near the ablation surface, where T is low and n high, it may be otherwise further away if the light is intense enough. To model the heat flux reasonably for such conditions, we introduce the usual flux-limit factor f. Although the model only considers one electron temperature at any given position and time, we find that two characteristic temperatures, corresponding to T_C (where saturation sets in) and T_H (at the critical surface), may be distinguished above a certain value of $I_0\lambda^4/\tau$.

2. BASIC EQUATIONS

To analyse the expanding plasma corona produced by irradiating a solid slab with laser light we follow Ref.[5], assuming one-dimensional geometry, quasi-neutral flow, high ion charge (to neglect ion pressure and internal energy), and absorption only within a thin layer around the critical density. The equations describing the expansion outside that layer are given by

$$\frac{Dn}{Dt} = -n\frac{\partial v}{\partial x} , \qquad \left(\frac{D}{Dt} = \frac{\partial}{\partial t} + v\frac{\partial}{\partial x} \right) \qquad (1)$$

$$\frac{m_i}{Z_i}\frac{n}{} \frac{Dv}{Dt} = -\frac{\partial}{\partial x}(nkT) \qquad (2)$$

$$nT\frac{D}{Dt}\left[k \ln \frac{T^{3/2}}{n} \right] = -\frac{\partial Q}{\partial x} \qquad (3)$$

The laser pulse incident from $x = \infty$ starts at $t = 0$, when the slab lies between $x = 0$ and, say, $x = -L$.

To take into account that the electron mean free path may be large over parts of the corona, we introduce a commonly used model for the heat flux Q:

$$Q = -Minimum \ (\ |Q_{Sp}| , |Q_{sat}|) \ sign\frac{\partial T}{\partial x} \qquad (4)$$

where $Q_{Sp} \equiv -\bar{K}T^{5/2} \partial T/\partial x$ is Spitzer's classical result and the saturated flux Q_{sat} is given by

$$Q_{sat} = -f\left(\frac{kT}{m_e} \right)^{1/2} nkT \ sign\frac{\partial T}{\partial x}$$

The appropriate value of the flux-limit factor f is still controversial [7].

The simplest, time-dependent, pulse

$$I(t) \equiv I_0 t/\tau , \qquad (0 < t < \tau)$$

greatly simplifies the analysis by leading to self-similar flow [4, 5]. Defining

$$v = n/n_R , \qquad Z = (\tau/t)^{2/3} T/T_R$$

$$y = \left(\frac{\tau}{t} \right)^{1/3} \frac{v}{v_R}, \quad \eta = \left(\frac{\tau}{t} \right)^{4/3} \frac{x}{x_R}, \quad q = \frac{\tau}{t}\frac{Q}{Q_R}$$

where the reference values are

$$T_R = (9k^2 Z_i \tau n_R /16 m_i \bar{K})^{2/3} \qquad (5)$$

$$v_R = \left[\frac{Z_i kT_R}{m_i} \right]^{1/2} , \qquad X_R = \frac{3}{4}\tau v_R$$

$$Q_R = \frac{3}{4}n_R kT_R v_R$$

Eqs (1) to (3) become

$$\frac{dv}{d\eta} = \frac{v}{\eta-y}\frac{dy}{d\eta} \qquad (6)$$

$$\frac{y}{4} - (\eta-y)\frac{dy}{d\eta} = -\frac{1}{v}\frac{d}{d\eta}(vz) \qquad (7)$$

$$v\left[z\left(1 + \frac{4}{3}\frac{dy}{d\eta} \right) - 2(\eta-y)\frac{dz}{d\eta} \right] = -\frac{dq}{d\eta} \qquad (8)$$

$$q = -Minimum \left[z^{5/2}\left|\frac{dz}{d\eta}\right| , \ \bar{f} v z^{3/2} \right]$$

$$\times \ sign \ \frac{dz}{d\eta} \qquad (9)$$

where $\bar{f} = 4/3(m_i/Z_i m_e)^{1/2} f [\cong 81f$ for $m_i = 2Z_i m_p]$.

For n_{cr} much less than solid density, the motion of both the ablation surface and the compressed medium at its left is slow compared with velocities in the corona so that, to analyse the expansion, this surface may be set at $\eta = 0$ ($x = 0$), the density there taking an infinite value. Then, choosing n_R appropriately, we have the boundary conditions

$$y = z = 0, \quad vz = 1 \quad at \quad \eta = 0 \qquad (10)$$

740

Let us note that Eqs (6) to (10) lead to a behaviour

$$z \simeq A\,\eta^{2/5}, \qquad \nu \simeq A^{-1}\,\eta^{-2/5}$$

$$y \simeq (3/25)\,A^{7/2}\,\eta^{2/5} \tag{11}$$

near $\eta \cong 0$. In addition, at the plasma-vacuum interface, which may lie at either finite or infinite distance, the mass, momentum, and energy fluxes must vanish,

$$\nu(y-\eta) \to 0,\ \nu z \to 0,\ q \to 0 \text{ as } \nu \to 0 \tag{12}$$

To analyse the thin, absorbing layer, we just integrate Eqs (1) to (3), written as conservation laws and including an absorption term in Eq.(3), across the layer to obtain jump conditions [8]:

$$\nu(y-\eta_{cr})\Big|_1^2 = 0 \tag{13}$$

$$\nu\left((y-\eta_{cr})^2 + z\right)\Big|_1^2 = 0 \tag{14}$$

$$\left[\nu(y-\eta_{cr})\left(\tfrac{5}{2}z + \tfrac{1}{2}(y-\eta_{cr})^2\right)\right.$$

$$\left.+\tfrac{3}{4}q\right]\Big|_1^2 = 6\nu_{cr}^2\,\bar{I}_o \tag{15}$$

where

$$\bar{I}_o = \left(\frac{4m_i}{9Z_i k}\right)^{3/2}\frac{\bar{K}\,I_o}{k^2 n_{cr}^2\,\tau} \tag{16}$$

Notice that the parameter α_c used in Refs [4, 5] is just $1/Z_i \bar{I}_o^{2/3}$. Subscripts 1 and 2 correspond to the overdense and underdense sides, respectively, so that $\nu_1 > \nu_{cr} > \nu_2$.

For $Q = Q_{Sp}$ everywhere, q, i.e. the temperature gradient, but not ν, y or z, would display jumps at η_{cr}; it was found [5] that then the entire flow (including the values of η_{cr}, ν_{cr}, A, etc.) could be determined for each value of $\bar{I}_o$. On the other hand, when using expression (4), jumps in the fluid variables must be allowed for, in general; since no analysis of the absorbing layer is carried out, an additional hypothesis may be needed to obtain a unique solution for each $\bar{I}_o$. Anyway, once this has been attained, Eqs (5) and (16) lead, at $t = \tau$, to

$$kT = \frac{m_i}{Z_i}\left(\frac{Z_i I_o}{m_i n_{cr}}\right)^{2/3}\frac{z}{(6\nu_{cr}\bar{I}_o)^{2/3}} \tag{17}$$

showing that any characteristic temperature is both proportional to $(I_o\lambda^2)^{2/3}$ and a function of $\bar{I}_o \propto I_o\lambda^2 \times \lambda^2/\tau$. Similarly, for the ablation pressure P_a, for example, we have $P_a = n_{cr}kT_{cr}/\nu_{cr}z_{cr}$.

3. LOW-INTENSITY LIMIT

A detailed discussion of the low-intensity $(\bar{I}_o \to 0)$ limit may help us to understand the general case, in the next section. It was shown in Refs [4, 5] that, for $\bar{I}_o$ small enough, the flow is isentropic for most of the corona, heat conduction being restricted to a thin (deflagration) layer that adjoins the ablation surface and encloses the absorption sublayer. To examine how the solution is affected by flux saturation, we just have to reconsider the structure of the deflagration layer. We must also keep in mind that the isentropic expansion must start at sonic (Chapman-Jouguet) or supersonic conditions (based on the isentropic sound speed) [4, 5].

Inside the deflagration layer, gradients are steep and the flow is quasi-steady. It is easy to see that this amounts to dropping η compared to y and taking $dy/d\eta$ to be large. Equations (6) to (8) can then be integrated once. Defining new (inner) variables given by

$$\left(\frac{\bar{\eta}}{\eta}\right)^{1/6} = \frac{\bar{y}}{y} = \left(\frac{\bar{\nu}}{\nu}\right)^{-1/2} = \left(\frac{\bar{z}}{z}\right)^{1/2} = \frac{\bar{q}}{q} = \frac{3A^{5/2}}{25}$$

where A is the constant in expression (11), Eqs (6) to (8), on integration, become

$$\bar{\nu} = \frac{1}{\bar{y}} \tag{18}$$

$$\bar{z} = \bar{y}(1 - \bar{y}) \tag{19}$$

$$\tfrac{1}{2}\bar{y}^2 + \tfrac{5}{2}\bar{z} + \tfrac{3}{4}\bar{q} = 0 \qquad (\bar{\eta} < \bar{\eta}_{cr}) \tag{20a}$$

$$= \sigma \qquad (\bar{\eta} > \bar{\eta}_{cr}) \tag{20b}$$

$$\bar{q}_{Sp} = -\bar{z}^{5/2}\,d\bar{z}/d\bar{\eta} \tag{21a}$$

$$\bar{q}_{sat} = -\bar{f}\left(\frac{\bar{z}^{3/2}}{\bar{y}}\right)\text{sign}\left(\frac{d\bar{z}}{d\bar{\eta}}\right) \tag{21b}$$

The left-hand side of Eqs (20) is a piece-wise constant, equal to zero in the overdense region because all three $\bar{y}$, $\bar{z}$ and $\bar{q}$ vanish at $\bar{\eta} = 0$; thus, on the overdense side,

$$\frac{1}{2}\bar{y}_1^2 + \frac{5}{2}\bar{z}_1 + \frac{3}{4}\bar{q}_1 = 0 \tag{22}$$

Then, writing condition (15) in inner variables, we find

$$\sigma = 6\bar{v}_{cr}^2 \bar{I}_0 \, (3A^{5/2}/25)^5 \tag{23a}$$

$$= \frac{1}{2}\bar{y}_2^2 + \frac{5}{2}\bar{z}_2 + \frac{3}{4}\bar{q}_2 \tag{23b}$$

Since the inner variables are of order unity, we have $A^{25/2}\bar{I}_0 = O(1)$ when $\bar{I}_0 \to 0$; the thickness of the deflagration, relative to the overal length of the corona, vanishes as $\bar{I}_0$. If Eq.(19) is used, the condition $\bar{y}^2/\bar{z} \geqslant 5/3$ for merging with the isentropic expansion becomes

$$\bar{y}_\infty \equiv \bar{y} \, (\bar{\eta} \to \infty) \geqslant \frac{5}{8} \tag{24}$$

Near $\bar{\eta} = 0$, the heat flux is always classical. If saturation occurs in the overdense flow, the corresponding value of $\bar{y}$ can be obtained from Eqs (19), (20a) and (21b) and is given by

$$\bar{f} = \frac{10}{3}\bar{y}^{1/2} \frac{1 - 4\bar{y}/5}{(1-\bar{y})^{3/2}} \tag{25}$$

On the other hand, the overdense, classical flow can not reach beyond $\bar{y} = 1/2$, because otherwise a multi-valued solution would ensue: $\bar{y}$ must increase with $\bar{\eta}$, but $\bar{z}$ has a maximum, $1/4$, at $\bar{y} = 1/2$ (where the isothermal Mach number, $M \equiv \bar{y}/\bar{z}^{1/2}$, is unity) [5, 6]. Hence, for all $\bar{f} > 4[\bar{y} > 1/2$ in expression (25)], there is no saturation and the solution is entirely classical. No discontinuities in the fluid variables are needed, and at the critical surface we have $\bar{y}_{1,2} = \bar{y}_{cr} = 1/2$, $\bar{z}_{1,2} = \bar{z}_{cr} = 1/4$, $\bar{v}_{1,2} = \bar{v}_{cr} = 2$. Again, the underdense flow can be shown not to reach beyond $\bar{y} = 5/8$; then, from condition (24), we obtain $\bar{y}_\infty = 5/8$, $\sigma = 25/32$, $\bar{q}_2 = |\bar{q}_1|/24 \ll |\bar{q}_1| = 1$ [6]. Using $\bar{z}_{cr}$, $\bar{v}_{cr}$, σ, Eq.(23a), and the relations $v/\bar{v} = \bar{z}/z \propto A^5$, we find $z_{cr}(v_{cr}\bar{I}_0)^{-2/3}$, independent of $\bar{I}_0$ in Eq.(17).

For $\bar{f} < 4$, we would have $\bar{y} < 1/2$ at saturation. The absorption sublayer must lie at the saturation point since otherwise the inequality $|\bar{q}_{sat}| < |\bar{q}_{Sp}|$ would hold for some distance, and use of (21b) in (20a) would yield $\bar{z} = const$, $\bar{q}_{Sp} = 0$, against the hypothesis. If the fluid variables were continuous, then $\bar{z}_{1,2} = \bar{z}_{cr} < 1/4$,

$\bar{y}_{1,2} = \bar{y}_{cr} < 1/2$, and $\bar{y}$ would decrease in the underdense flow. Hence, discontinuities must be allowed for, and, as previously pointed out, some assumptions will be required to make the solution unique:

a) First, remark that the three conservation laws (18) to (20) might involve jumps in four quantities, $\bar{v}$, $\bar{y}$, $\bar{z}$ and $\bar{q}$ (outside a shock, in an ideal fluid, there are no transport terms, and only three quantities are involved in the jumps). Now, for $\bar{q} = \bar{q}_{Sp} \propto d\bar{z}/d\bar{\eta}$ at conditions 1 and 2, one should clearly have $\bar{z}_2 = \bar{z}_1$, if $\bar{q}$ is to remain finite. But the fact that heat conduction is important outside the thin absorption sublayer means that, in a sense, the electron mean free path is large. This is the more so at saturation; hence we should have $\bar{z}_2 = \bar{z}_1$, in all cases. We recall here the somewhat similar case of an isothermal viscous shock [9].

It is easy to verify that the structure of the deflagration layer would admit an isothermal jump at points where $\bar{q} = \bar{q}_{Sp}$; that is, at any $\bar{y} < 1/2$ for $\bar{f} > 4$, and at any $\bar{y}$ less than the value in (25) for $\bar{f} < 4$. To make the solution unique, we use the following argument: in an isothermal discontinuity, we have $\bar{y}_2 = 1 - \bar{y}_1$, and also $M_2 = 1/M_1 > 1$. Now, Eqs (22) and (23) when added and rewritten in dimensional form, read

$$I + Q_1 - Q_2 = n_1 v_1 kT \left[\frac{1}{2}M_2^2 - \frac{1}{2}M_1^2\right]$$

where $n_1 v_1$ is the electron flux. The entropy jump per electron is $k \ln (n_1/n_2)$ or $k \ln (M_2/M_1)$. The laser irradiance I and the net heat flux $Q_1 - Q_2$ account for part of that jump, but clearly there must exist an additional source of entropy of the following value:

$$n_1 v_1 k \ln (M_2/M_1) - n_1 v_1 k \frac{1}{2} (M_2^2 - M_1^2)$$

$$\equiv \frac{1}{2} n_1 v_1 k \left[\ln (M_1^2)^2 + M_1^2 - \frac{1}{M_1^2}\right]$$

per unit area and time. The last bracket is positive (negative) for $M_1 > 1$ ($M_1 < 1$). For an isothermal viscous shock ($M_1 > 1$), viscosity accounts for the additional entropy generation. Here, however, $M_1 < 1$, so that entropy 'dissipation' would be needed. This is impossible in a collision-dominated medium.

Thus, we confirm that for $\bar{f} > 4$ absorption occurs at $\bar{y} = 1/2$, where all three $\bar{v}$, $\bar{y}$ and $\bar{z}$ are continuous, while for $\bar{f} < 4$ absorption occurs at saturation, only $\bar{z}$ being continuous; at saturation, collisions are infrequent, and even the concept of entropy per
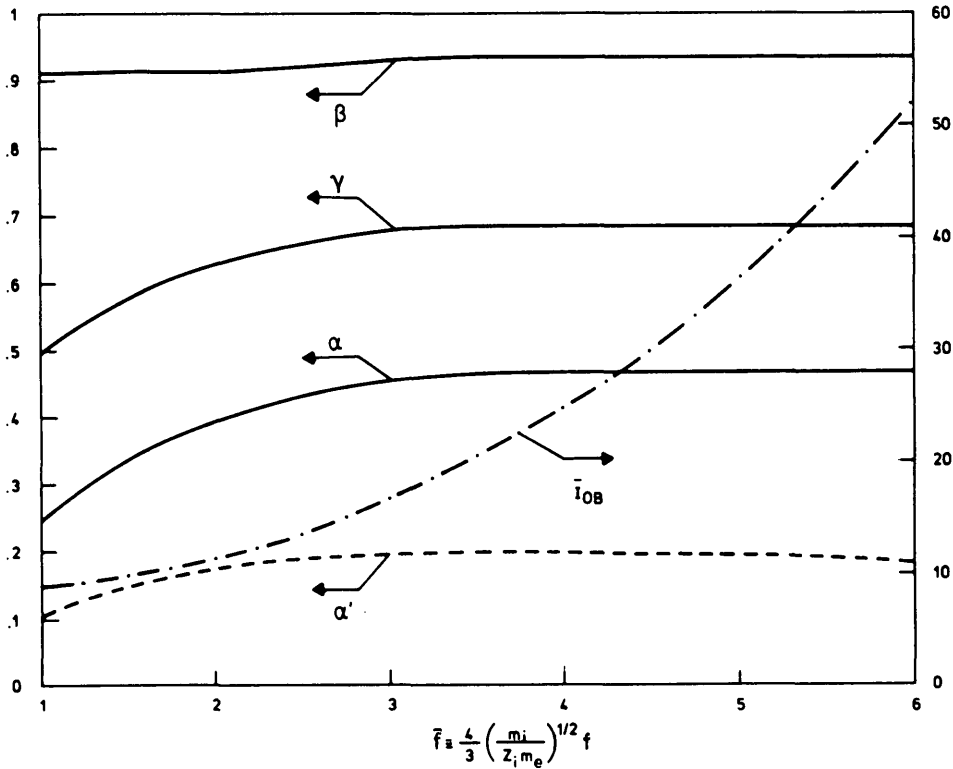
FIG.1. Dependence of various quantities on the flux-limit factor f: α, β, γ defined in Eqs (26); value of $\bar{I}_0$, as defined in Eq.(16), above which there is saturated overdense flow; α' defined in Eq.(38).

electron, k ln $(T^{3/2}/n)$, is of doubtful value. Furthermore, for the general case $(\bar{I}_0$ not small) of the next section, when saturation applies to part of the overdense flow, we are led to the hypothesis that the isothermal jump, when required, will appear where entropy dissipation would be minimum, that is, for M_1 as close to unity as possible.

b) Second, an ad hoc assumption on $\bar{\nu}_{cr}$ is needed; $\bar{\nu}_{cr}$, though appearing in (23a), nowhere enters the analysis. Since $\bar{\nu}_2 \leqslant \bar{\nu}_{cr} \leqslant \bar{\nu}_1$, we may write $\bar{\nu}_{cr} = \bar{\nu}_1 \phi$ $(\bar{\nu}_2/\bar{\nu}_1)$ where $s \leqslant \phi(s) \leqslant 1$. We used both $\phi = (\bar{\nu}_2/\bar{\nu}_1)^{1/2}$ and $\phi = (1 + \bar{\nu}_2/\bar{\nu}_1)/2$ in our computations to check for differences; the agreement was good, except for $\bar{\nu}_2/\bar{\nu}_1$ very small.

We can now go back to the analysis of the deflagration layer for $\bar{f} < 4$. For $\bar{f} \rightarrow 0$ in (25), $\bar{y}_1 \rightarrow 0$ and $\bar{y}_2 \rightarrow 1$. One can show that if

$$\bar{y}_2 < \frac{5}{8} \quad \left[\bar{f} > 56/5(15)^{1/2}\right]$$

the underdense flow takes $\bar{y}$ from $\bar{y}_2$ to 5/8, and

$\sigma = 25/32$ as before; if $\bar{f} < 56/5(15)^{1/2}$, all three $\bar{\nu}$, $\bar{y}$ and $\bar{z}$ are constant in the underdense flow and $\sigma = (5y_2 - 4y_2^2)/2$, the isentropic expansion starting supersonic.

Final results for critical temperature T_{cr}, ablation pressure P_a, and mass ablation rate $\dot{m}_a$, when $\bar{I}_0$ is small, are

$$T_{cr} = \alpha(\bar{f}) \frac{m_i}{Z_i} \left[\frac{Z_i I_o}{m_i n_{cr}}\right]^{2/3} \tag{26a}$$

$$P_a = \beta(\bar{f}) \, n_{cr} \frac{m_i}{Z_i} \left[\frac{Z_i I_o}{m_i n_{cr}}\right]^{2/3} \tag{26b}$$

$$\dot{m}_a = \gamma(\bar{f}) \, n_{cr} \frac{m_i}{Z_i} \left[\frac{Z_i I_o}{m_i n_{cr}}\right]^{1/3} \tag{26c}$$

where α, β, γ, given in Fig.1, are independent of $\bar{I}_0$.

4. ARBITRARY INTENSITY

When $\bar{I}_0$ is not small, heat conduction is important throughout the expanding corona. As was shown in the last section, the coefficient A in (11) decreases for $\bar{I}_0$ increasing; the evolution of the flow as $\bar{I}_0$ increases may be also discussed in terms of decreasing A. It is clear that once a value of A is chosen the numerical integration of Eqs (6) to (9) can proceed from η equal to zero; note that the isothermal Mach number in a frame tied to the local values of the fluid variables, $M \equiv (y - \eta)/z^{1/2}$ is always subsonic for small η.

Consider now the range $\bar{f} < 4$. For $\bar{I}_0$ small (A large), heat saturation occurred at a Mach number still subsonic (Section 3). Numerically we find that this remains true as $\bar{I}_0$ keeps increasing, the Mach number at saturation $M_{sat}(\bar{f}, \bar{I}_0)$ decreasing all along. Further, we find analytically that a function $M_*(\bar{f})$ exists such that an overdense, saturated flow cannot exist for $M_* < M < 1$; we show that $M_{sat}(\bar{f}, 0)$, which follows from (19) and (25) and is given by

$$3\bar{f} = 10 M_{sat}(1 + M_{sat}^2/5) \qquad (27)$$

is larger than M_* for all $\bar{f}$. Therefore, we conclude that for $\bar{I}_0$ below some value $\bar{I}_{0B}(\bar{f})$ we have $M_{sat} > M_*$; absorption must occur at saturation where an isothermal jump takes M from $M_1 \equiv M_{sat}$ to $M_2 \equiv 1/M_{sat}$. This is naturally the small-$\bar{I}_0$ case of Section 3. On the other hand, for $\bar{I}_0 > \bar{I}_{0B}$ we have $M_{sat} < M_*$, and a region of saturated, overdense flow exists, which increases M from M_{sat} to its largest possible value M_*, where the isothermal jump to $1/M_*$ occurs.

For $\bar{f} > 4$, the flow at small $\bar{I}_0$ becomes sonic before saturation; absorption occurs at the sonic point, where the fluid variables are continuous (Section 3). This situation persists as $\bar{I}_0$ increases until a value is reached for which saturation sets in at sonic conditions. For larger $\bar{I}_0$, the discussion just developed for $\bar{f} < 4$ applies.

Hence, for all $\bar{f}$, an overdense region of saturated flow exists when $\bar{I}_0$ is above some value $\bar{I}_{0B}(\bar{f})$, and then two characteristic temperatures may be distinguished, that at saturation and that at the critical surface.

We now prove the statements about $M_*(\bar{f})$. For $q = q_{sat} \equiv -\bar{f}\nu z^{3/2}$ (overdense flow, $dz/d\eta > 0$), we may rewrite Eqs (6) to (8) introducing phase-space variables:

$$Y = \frac{y - \eta}{\eta}, \qquad \theta = \frac{z}{\eta^2}, \qquad N = \frac{\nu}{\eta^3} \qquad (28)$$

that yield a decoupled equation for $\theta(Y)$:

$$\frac{d\theta}{dY} = \frac{\Delta_o}{\Delta_\infty} \qquad (29)$$

$$\Delta_o = \bar{f}\theta^{5/2} - \frac{3 + 20Y}{3}\theta^2 - \bar{f}\frac{1 + Y + 12Y^2}{4}\theta^{3/2}$$

$$- \frac{1 - 2Y - 12Y^2}{3} Y\theta \qquad (30)$$

$$\Delta_\infty = \bar{f}\frac{1 + Y}{2}\theta^{3/2} - \frac{10Y + 13}{3}Y\theta$$

$$- \frac{Y}{2}(1 + Y)(1 + 4Y)\left(\bar{f}\frac{3}{4}\theta^{1/2} - Y\right) \qquad (31)$$

$N(Y)$, $\eta(Y)$ are then given by

$$\frac{dN}{dY} = \frac{-N}{Y}\frac{\Delta_\infty + (1 + 4Y)\Delta_s}{\Delta_\infty} \qquad (32)$$

$$\frac{d\ln\eta}{dY} = \frac{\Delta_s}{\Delta_\infty} \qquad (33)$$

where

$$\Delta_s = -\bar{f}\frac{\theta^{3/2}}{2} + \frac{10}{3}Y\theta + \bar{f}\frac{3}{2}Y^2\theta^{1/2} - 2Y^3 \qquad (34)$$

In the new variables, the Mach number becomes $M \equiv Y/\theta^{1/2}$; the line $\Delta_s = 0$ in the Y, θ plane is a parabola:

$$\bar{f} = \frac{20}{3} M \frac{1 - 3M^2/5}{1 - 3M^2} \qquad (35)$$

For any $\bar{f}$, Eq.(35) has two roots, but only one, called $M_*(\bar{f})$, is subsonic. Using (28) to (29) and (33), we obtain

$$\frac{dz}{d\ln\eta} = -\frac{\theta^2}{\Delta_s}\left[1 - \frac{2}{3}M^2 + \frac{M}{3\theta^{1/2}}\right.$$

$$\left. + \frac{\bar{f}}{4}\left(M + \frac{1}{\theta^{1/2}}\right)\right] \qquad (36)$$

For $M_* < M < 1$, both Δ_s and the bracket in (36) are positive, so that a contradiction, $dz/d\eta < 0$, follows.

Furthermore, a comparison of (27) and (35) shows that for small $\bar{f}$, $M_{sat}(\bar{f}, 0) \cong 2M_*(\bar{f}) > M_*(\bar{f})$. Since the equation $M_{sat}(\bar{f}, 0) = M_*(\bar{f})$,

$$\frac{10}{3} M \left(1 + \frac{M^2}{5}\right) = \frac{20}{3} M \frac{1 - 3M^2/5}{1 - 3M^2}$$

has no positive roots, we conclude that $M_{sat}(\bar{f}, 0) > M_*(\bar{f})$ for all $\bar{f}$, as was pointed out previously.

Once η_{cr} and quantities with subscript 1, are known for each A, Eq.(15) would yield $\bar{I}_0$, and, finally, T_M, P_a, and $\dot{m}_a$, if q_2 is known and the function ϕ in $\nu_{cr} = \nu_1 \phi(\nu_2/\nu_1) \equiv \nu_1\phi(M_1^2)$ has been chosen. For $M_1 = 1$, we would have

$$\bar{I}_0 = (q_2 - q_1)/8\nu_{cr}^2 \qquad (37a)$$

while, for $M_1 < 1$,

$$\bar{I}_0 = \frac{q_2}{8\nu_{cr}^2} + \frac{M_1\nu_1 z_{cr}^{3/2}}{\nu_{cr}^2}\left[\frac{\bar{f}}{8M_1} + \frac{M_1^{-2} - M_1^2}{12}\right] \qquad (37b)$$

where $M_1 \equiv M_{sat}(\bar{f}, A)$ for $M_{sat} > M_*(\bar{f})$, and $M_1 \equiv M_*$ for $M_{sat} < M_*$. To determine q_2, one should analyse the underdense region, as in Section 3; this is discussed in the Appendix. However, in Section 3, and for $M_1 = 1$, q_2 was found to be much less than $|q_1|$, so that neglecting q_2 in (37) would yield an error of no more than a few per cent. Calculations including an analysis of the underdense flow have, for a variety of conditions, left little doubt that $q_2 \ll |q_1|$, in all cases. Then, expressions (37a) or (37b) yield $\bar{I}_0$ by themselves. For $M_1 \equiv M_*$ ($\bar{I}_0 > \bar{I}_{0B}$), expression (37b) shows that $z_{cr}/(\nu_{cr}\bar{I}_0)^{2/3}$ is a constant (independent of $\bar{I}_0$) for each $\bar{f}$, as in the small-$\bar{I}_0$ case,

$$kT_{cr} = \alpha'(\bar{f})(m_i/Z_i)(Z_i\bar{I}_0/m_i n_{cr})^{2/3} \qquad (38)$$

For $\bar{I}_0$ large, the temperature at saturation, the ablation pressure, etc. take a simple form, too. Note that Eq.(29) has a saddle point P (Fig.2) where $\Delta_0 = 0$ and $\Delta_\infty = 0$ meet. The figure shows integral curves for (29), including those (L_1, L_2) passing through P. For $M_{sat} < M_*$, the saturation point approaches L_1 as A keeps decreasing, so that the solution reaches the jump line $\Delta_s = 0$ ($M = M_*$) after passing close to P. It may be shown that the solution acquires an asymptotic form, for $\bar{I}_0 \to \infty$,

$$P_a \propto n_{cr} kT_{cr}\bar{I}_0^{\frac{1-Y_P}{1+4Y_P}}$$

$$kT \text{ (at saturation)} \propto kT_{cr}\bar{I}_0^{-\frac{2Y_P}{1+4Y_P}}$$

where Y_P is the Y co-ordinate of P.
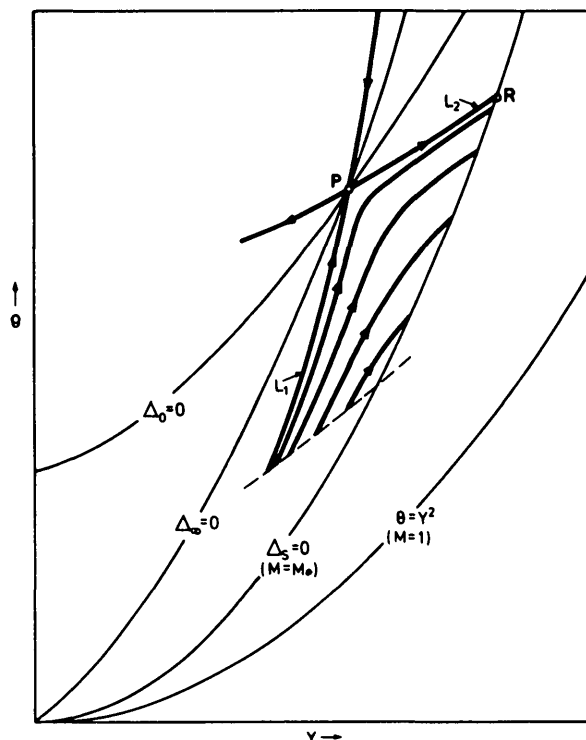
FIG.2. Phase-plane schematics of Eq.(29) for overdense saturated flow. Each integral curve goes from the saturation point (dashed line) to the isothermal jump at the $M = M_*$ line.

5. DISCUSSION

The behaviour of the plasma corona ejected by a solid slab irradiated with a laser pulse of maximum intensity I_0, wavelength λ, and rise-time τ, is governed by a dimensionless parameter $\bar{I}_0 \propto I_0\lambda^4/\tau$, defined in Eq.(16) [4, 5]. For $\bar{I}_0$ below a certain value $\bar{I}_{0B}$, heat conduction is classical everywhere, while for $\bar{I}_0 > \bar{I}_{0B}$ the overdense part of the corona exhibits a region of classical heat flux next to the ablation surface and a region of saturated heat flux adjoining the critical
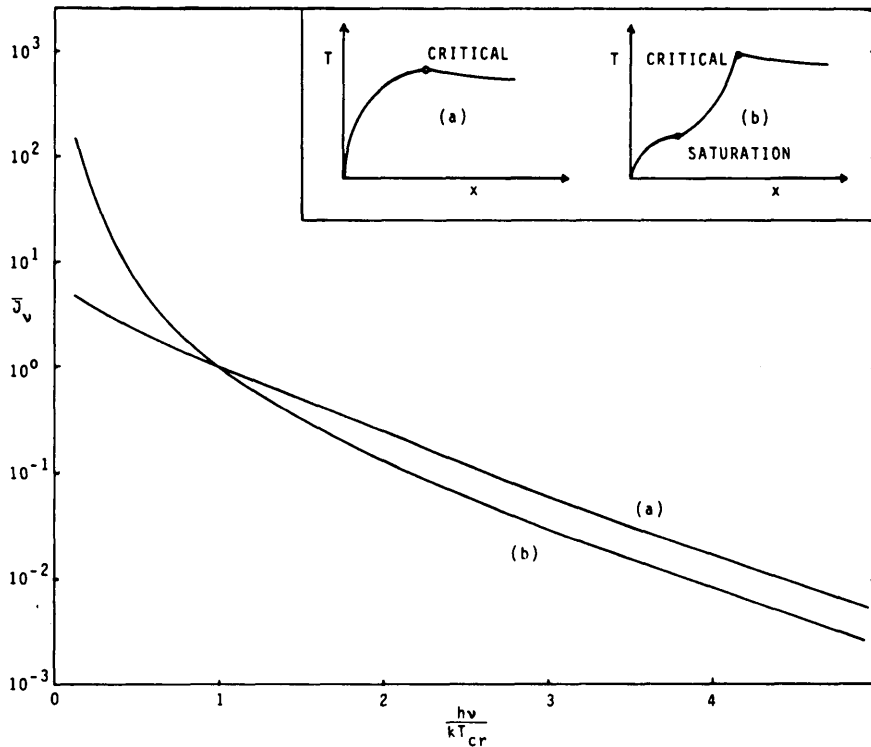
FIG.3. Overall bremsstrahlung power spectrum $\bar{J}_\nu$ for representative classical (a) and classical-saturated (b) overdense conditions. Insert: schematic temperature profiles for cases (a) and (b).

surface; $\bar{I}_{0B}$, as given in Fig.1, is a function of the usual flux-limit factor f. Temperature profiles for both cases are shown schematically in Fig.3.

We can speak of one or two characteristic temperatures, according to the case. To make this point clear, consider, for example, the bremsstrahlung power emitted at frequency ν, per unit volume and frequency, at any point of the plasma [10]:

$$J_\nu \propto n^2 T^{-1/2} \exp\left(-h\nu/kT\right)$$

Radiation from the entire plasma would involve the integral

$$\bar{J}_\nu \equiv \int_0^\infty J_\nu \, dx/x_{cr}$$

represented in Fig.3 for particular examples of the two opposite cases. The curve log $\bar{J}_\nu$ versus ν, used for plasma diagnostics, would be straight for an isothermal plasma, and it is nearly so in case (a); in case (b), on the other hand, the slope and, therefore, the temperature change from values close to the temperature at saturation to values close to the critical temperature.

We shall now identify these two temperatures with the experimentally observed hot-(T_H) and cold-(T_C) electron temperatures, respectively. In Figs 4 and 5, we compare our quantitative results for T_H and T_C with data compiled in Ref.[3] from a large number of Nd and CO_2 experiments. Several points should be noticed:

i) The agreement is best for $f \cong 0.03$ (and very poor for no flux inhibition, $f \cong 0.6$), a conclusion reached previously in different ways.

ii) The agreement is reasonably good, considering the simplicity of the model: to compute the temperatures for given I_0 and λ (or n_{cr}), one has to find $\bar{I}_0$, choosing values for both Z_i and the Coulomb logarithm in $\bar{K}$, the rise-time τ, and the fraction of laser energy absorbed, which will differ from one experiment to another. For Nd and low values of I_0, the fractional absorption of 0.5 used in Fig.4 may be an underestimate, which may explain the low temperatures predicted by the theory; also the appropriate value of f for low intensity and short wavelength could be larger than 0.03, improving again the agreement at low I_0.

iii) Rise-time effects are crucial. As was noted in the introduction, a quasi-steady analysis of the region between the ablation and the critical surfaces as in
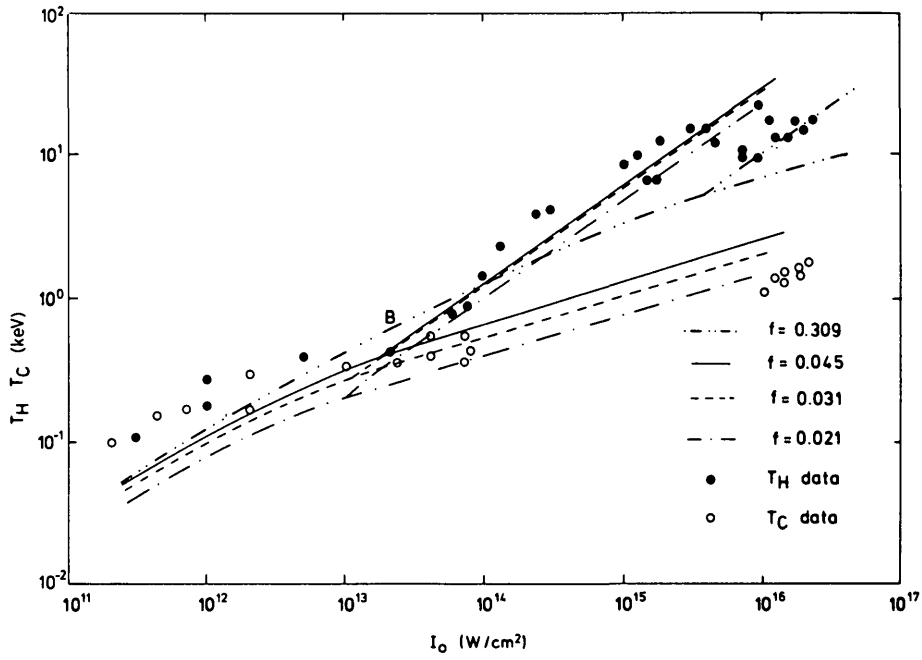
FIG.4. Hot and cold temperatures versus light intensity from theory and a variety of experiments with Nd lasers; to compute the theoretical curves, we set $Z_i = 4$, $m_i/Z_i = 2 \times$ proton mass, Coulomb logarithm = 8, $\tau = 0.3$ ns, fractional absorption = 0.5. B is the bifurcation point.
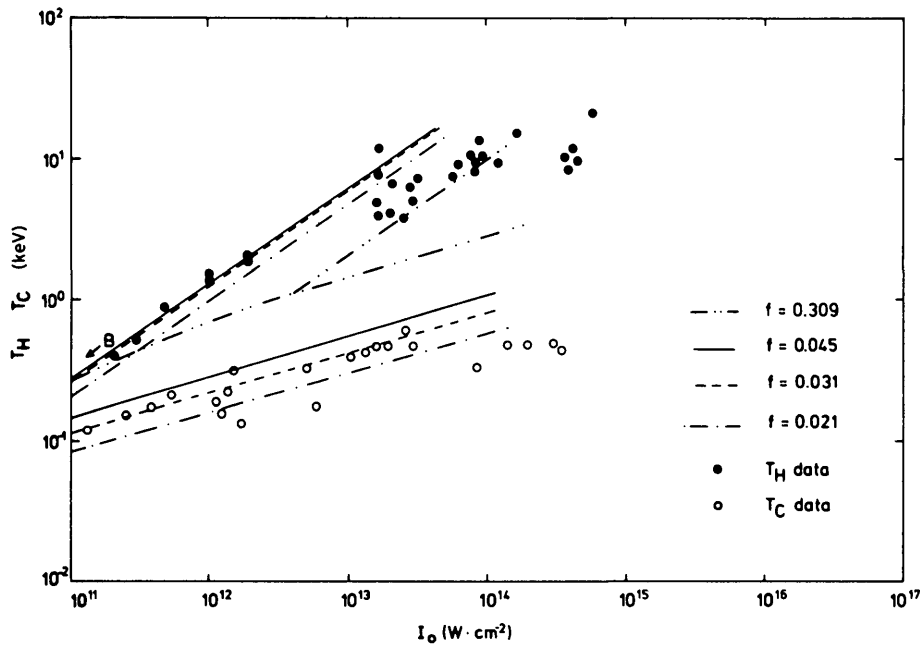
FIG.5. Hot and cold temperatures versus light intensity from theory and a variety of experiments with CO_2 lasers; all quantities as in Fig.4, except $\tau = 3$ ns.
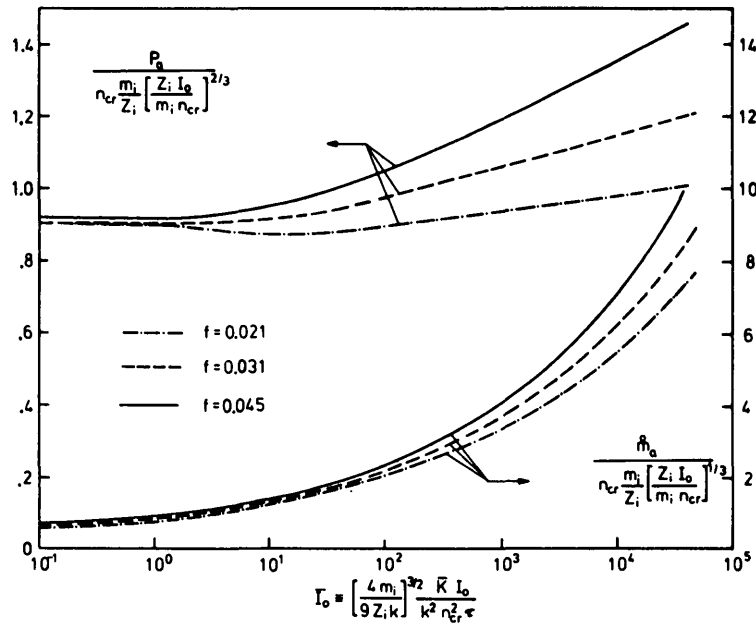
FIG.6. Dimensionless ablation pressure and mass ablation rate versus dimensionless laser intensity.

Section 3 (basically implying negligible heat capacity for that region) would yield a universal curve $T_M/(I_0\lambda^2)^{2/3} =$ const. It is , however, clear that the values of temperature and $I_0\lambda^2$ at the bifurcation point B are different in Figs 4 and 5; again, the data for $T_C(I_0\lambda^2)$ from the figures do not fall into a universal curve. In fact, a quasi-steady analysis of the ablation region, yielding a universal structure and a scaling law, could never predict the qualitative changes occurring at point B. (For spherical geometry in quasi-steady conditions [8], the finite radius of the pellet plays a role similar to that of time in our planar case.) Note, finally, that the quasi-steady prediction for T_M above point B is about 2.5 times larger than T_H as given by our analysis [compare α and α' in Fig.1, and Eqs (26a) and (38)].

iv) The experimental data show the slope of T_H changing when $T_H \sim 10T_C$ and $I_0\lambda^2 \cong 10^{15}\,W\cdot\mu m^2 \cdot cm^{-2}$; for higher intensities, T_H/T_C remains close to 10. (We call attention to the fact that a plasma expansion with two uniform electron temperatures and free of singularities cannot exist for $T_H/T_C > 5 + (24)^{1/2} \cong 10$ [11].) Our analysis does not predict such a change. This is reasonable because, for $I_0\lambda^2 > 10^{15}$, roughly, hot-electron generation, mainly due to resonant absorption, is expected to be substantial [12]; that is, for such $I_0\lambda^2$ values there would really be two temperatures at each

point of the plasma, violating our one-temperature assumption. Our analysis applies to the range $I_0\lambda^2 < 10^{15}$ and explains why two temperatures are observed starting around $10^{13}\,W\cdot\mu m^2 \cdot cm^{-2}$, when hot-electron generation would appear to be negligible. To distinguish experimentally between our 'two' temperatures and the real two temperatures of Refs [12], measurements with good spatial resolution would be needed.

We give the ablation pressure and the mass ablation rate in Fig.6, in dimensionless form, for future reference.

Appendix

It is possible to show that near the plasma-vacuum boundary the heat flux is always classical. Thus, we introduce new phase-space variables [5]

$$Y = \frac{y-\eta}{\eta}, \qquad N = \frac{\upsilon}{\eta^3}$$

$$\theta = \frac{z}{\eta^2}, \qquad F = \frac{q}{\eta^6}$$

leading to the equations

$$\frac{d\theta}{dY} = \frac{2\theta + F/\theta^{5/2}}{Y+1} \frac{\Delta_1}{\Delta_2}$$

$$\frac{d \ln \eta}{dY} = -\frac{1}{Y+1} \frac{\Delta_1}{\Delta_2}$$

$$\frac{d \ln N}{dY} = \frac{1}{Y}\left(\frac{4Y+1}{Y+1}\frac{\Delta_1}{\Delta_2} - 1\right)$$

$$\frac{dF}{dY} = \frac{6F+N\left((4Y+7)\theta/3+2FY/\theta^{5/2}\right)}{Y+1}\frac{\Delta_1}{\Delta_2} - \frac{4}{3}N\theta$$

$$\Delta_1 = \theta - Y^2$$

$$\Delta_2 = \theta - Y\left(Y+\frac{1}{4} - \frac{F}{\theta^{5/2}(Y+1)}\right)$$

At the plasma boundary, $Y = 0$, we must have $N = F = \theta = 0$ ($\theta \cong Y/4$); clearly, the flow is subsonic for Y low enough.

On the other hand, we have found in Sections 3 and 4 that the Mach number on the underdense side (2) of the absorbing layer was either sonic or supersonic. Consequently, the underdense solution must cross the sonic line. We found that this may happen in either of two ways: 1) the solution crosses the sonic line through a singular point at that line, i.e. the case found for everywhere classical flow [5]; 2) a shock appears where the Mach number goes from supersonic to subsonic; we have assumed the shock to be isothermal and used the jump conditions (13) − (15) with $\bar{I}_0 = 0$.

In particular, for $\bar{I}_0 \to \infty$, always a shock appears. If, in addition, $\bar{f} < 1.5$, the flow beyond the absorption layer is first saturated and then classical ahead of the shock, and again saturated and finally classical behind the shock. For $1.5 < \bar{f} < 2.9$, the flow is everywhere classical behind the shock, and for $\bar{f} > 2.9$ the entire underdense flow is classical.

It was found in Ref.[5], where saturation was not considered, that for large $\bar{I}_0$ the entire corona was subsonic. We found here that this may also happen if f is large enough (about 0.6 and above) and $\bar{I}_0$ large but below a certain value.

ACKNOWLEDGEMENT

REFERENCES

[1] GIOVANIELLI, D.N., Bull. Am. Phys. Soc. Ser. II 9 (1976) 1047.

[2] LINDMAN, E.L., J. Phys. 38, Supplement Fasc. 12 (1977) C6–9.

[3] YAMANAKA, C., Nucl. Fusion 20 (1980) 507.

[4] SANMARTÍN, J.R., BARRERO, A., Phys. Fluids 21 (1978) 1957.

[5] BARRERO, A., SANMARTÍN, J.R., Plasma Phys. 22 (1980) 617.

[6] SANZ, J., LIÑÁN, A., RODRIGUEZ, M., SANMARTÍN, J.R., Phys. Fluids 24 (1981) 2098.

[7] BRAITHWAITE, N. St. J., MONTES, A., WICKENS, L.M., Plasma Phys. 23 (1981) 713.

[8] MAX, C.E., McKEE, C.F., MEAD, W.C., Phys. Fluids 23 (1980) 1620.

[9] LANDAU, L.D., LIFSHITZ, E.M., Fluid Mechanics, Pergamon Press, New York (1966) Ch.88.

[10] SHAY, H.D., HAAS, R.A., KRUER, W.L., BOYLE, M.J., PHILLION, D.W., et al., Phys. Fluids 21 (1978) 1634.

[11] WICKENS, L.M., ALLEN, J.E., J. Plasma Phys. 22 (1979) 167.

[12] FORSLUND, D.W., KINDEL, J.M., LEE, K., Phys. Rev. Lett. 39 (1977) 284; ESTABROOK, K., KRUER, W.L., Phys. Rev. Lett. 40 (1978) 42.